ELSEVIER

Atmospheric Environment 38 (2004) 6253–6261

ATMOSPHERIC ENVIRONMENT

www.elsevier.com/locate/atmosenv

Heterogeneous chemistry of individual mineral dust particles from different dust source regions: the importance of particle mineralogy

B.J. Krueger[a], V.H. Grassian[a,*], J.P. Cowin[b], A. Laskin[b,1]

[a]*Department of Chemistry and the Center for Global and Regional Environmental Research, University of Iowa, Iowa City, IA 52242, USA*

[b]*William R. Wiley Environmental Molecular Sciences Laboratory, Pacific Northwest National Laboratory, P.O.Box 999, MSIN K8-88, Richland, WA 99352, USA*

Abstract

The heterogeneous chemistry of individual dust particles from four different dust source regions is investigated on a particle-by-particle basis using state-of-the-art scanning electron microscopy techniques including computer-controlled Scanning Electron Microscopy/Computer-Controlled energy dispersive X-ray (CCSEM/EDX) analysis. Morphology and compositional changes of individual particles as they react with nitric acid are observed. Clear differences in the reactivity of mineral dusts from these four different dust regions with nitric acid could be observed. Mineral dust from source regions containing high levels of calcium, such as those found in parts of China and Saudi Arabia, are found to react to the greatest extent. Calcium containing minerals, such as calcite ($CaCO_3$) and dolomite ($CaMg(CO_3)_2$), react to form nitrate salts whereas other calcium containing minerals such as gypsum ($CaSO_4 \cdot 2H_2O$) do not react. The importance of particle chemical composition and mineralogy in the heterogeneous chemistry of mineral dust aerosol is definitively borne out in this study of individual dust particles.

Keywords: Heterogeneous chemistry; Mineral aerosol; Atmospheric processing; Particle analysis

1. Introduction

Mineral dust aerosol makes up a large fraction of the tropospheric aerosol mass and therefore impacts the Earth's climate and the atmospheric environment in several ways. First, mineral dust aerosol influences climate through direct and indirect climate forcing by scattering and absorbing incoming solar radiation and by nucleating clouds (Tegen, 2003; Buseck and Pósfai, 1999). Second, mineral dust aerosol influences biogeochemical cycles as iron-containing minerals provide an important nutrient for ocean life (Zhu et al., 1993). Third, mineral dust in the respirable size range is deleterious to human health (Guthrie, Jr. and Mossman, 1993). Finally, mineral dust aerosol influences the chemistry of the Earth's atmosphere by reducing photolysis rates of gas-phase species due to the fact that dust can decrease the incident solar flux and through heterogeneous chemistry (Bian and Zender, 2003; Tang et al., 2004).

*Corresponding author. Tel.: +1-319-335-1392; fax: +1-319-353-1115.

E-mail addresses: vicki-grassian@uiowa.edu (V.H. Grassian), alexander.laskin@pnl.gov (A. Laskin).

[1]Tel.: +1-509-376-8741; fax: +1-509-376-6066.

1352-2310/$ - see front matter © 2004 Elsevier Ltd. All rights reserved.
doi:10.1016/j.atmosenv.2004.07.010

Heterogeneous chemistry of mineral dust is not only intimately linked to the impact that dust has on the gas-phase composition of the atmosphere it can also influence how mineral dust aerosol impacts climate, biogeochemical cycles and health. For example, as mineral dust reacts in the atmosphere the physicochemical properties of the particles change including the optical properties of the particles and their effectiveness to serve as cloud condensation nuclei (Martin, 2000). This is important as there is increasing evidence that mineral dust aerosol impacts cloud formation, cloud properties and precipitation (Levin et al., 1996; Rosenfeld et al., 2001; Yin et al., 2002; Rudich et al., 2002; Sassen et al., 2003; Toon, 2003; Mahowald and Kiehl, 2003; Rudich et al., 2003). In addition, the bioavailability of iron in iron-containing dust particles may differ after the particles react with trace gases, especially acidic gases, in the atmosphere (Meskhidze et al., 2003). Finally, as particles age in the atmosphere they can become coated with carcinogens from the uptake of compounds such as polycyclic aromatic hydrocarbons (Garçon et al., 2000). Once coated, these particles are potentially even more of a health concern. Thus, an increased understanding of the chemistry of mineral dust is warranted.

Although mineral dust aerosol is often discussed as a single entity aerosol, similar to sea salt, it should be immediately obvious that this is a poor representation of the rich mineralogy and varying chemical composition of the dust. Not only is the mineralogy of the dust rich it is also source specific (Claquin et al., 1999). Thus, when atmospheric chemistry or global climate models represent mineral dust aerosol as a size distribution with a single kinetic parameter for reaction with a particular trace gas (Dentener et al., 1996; Bian and Zender, 2003; Liao et al., 2003; Martin et al., 2003; Bauer et al., 2004) or a single refractive index to model climate forcing (Dickerson et al., 1997), the results of these calculations can be called into question.

Here we present a case study of the heterogeneous chemistry of mineral dust with nitric acid, an important trace atmospheric gas. The composition and corresponding chemistry of individual particles from four different dust sources including China Loess from Asia, Saharan Sand from Africa and coastal and inland dust from Saudi Arabia have been investigated. The map shown in Fig. 1 identifies the source regions of these different dust samples. Several of these regions have been identified as being in the "dust belt". The "dust belt" consists of the largest and most persistent sources of dust in the world (Prospero et al., 2002) Digital images of the powdered samples are also shown in Fig. 1. The chemistry of individual dust particles was analyzed with Scanning Electron Microscopy (SEM) and Energy Dispersive X-ray (EDX) analysis. As discussed in detail below, the data show that the reactivity of nitric acid with mineral dusts is dust source dependent because of the varying mineralogy of the

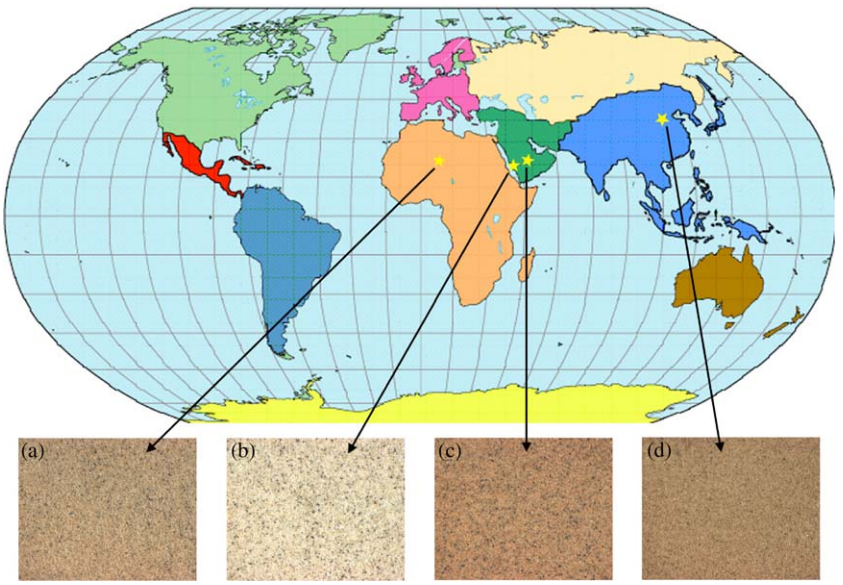

Fig. 1. The world map identifies the locations of the different mineral dust sources used in this study. Table 1 lists the chemical compositions of these four samples: (a) Saharan Sand; (b) Coastal Saudi Sand; (c) Inland Saudi Sand; and (d) China Loess. Each of these samples were exposed to nitric acid vapor, a trace gas in the atmosphere, and the different reactivities were followed with SEM and EDX (see text for further details). Digital pictures of the different mineral dusts from each source region are also shown.

different dust sources. We show that calcium-containing carbonate particles, including calcite and dolomite, react to the greatest extent with nitric acid to form nitrate salts. These particles show unique morphological changes upon reaction and a change in hygroscopicity of the particle after reaction. Reactions of these particles are not surface limited and continued consumption of the available carbonate is observed (Krueger et al., 2003a,b). As a result, calcium-containing carbonate particles are converted into aqueous droplets of nitrate salts following the reaction. Other calcium-containing particles such as gypsum ($CaSO_4 \cdot 2H_2O$) are not observed to be reactive. Quartz and aluminum silicate clays, a large component of the mineral dust, appear less reactive, at least with respect to bulk reactivity of the particle. Importantly, the results of this study indicate substantial differences in individual particle reactivity and therefore clearly show the need to include dust mineralogy in atmospheric chemistry and climate models.

2. Experimental methods

To obtain particles of atmospherically relevant sizes, the samples of sand from different source regions were first sieved to $<40\,\mu m$ particle sizes and then dispersed onto TEM grids for analysis and chemical processing. TEM grids, coated with a thin ($\sim$50 nm) carbon film, were purchased from Ted Pella, Inc. (Carbon Type-B on Au 200 grid) and used as substrates in this work. Once the particles were dispersed onto the grids, the larger particles and particles that poorly adhered to the grid were mechanically removed using compressed air. The mean diameter of the deposited particles was in the order of $\sim$0.7 μm. The particle density was 5000–10,000 particles mm^{-2} of the substrate area. The separation distance between single particles was typically $\sim$1–5 μm.

A FEI XL30 digital field emission gun Environmental Scanning Electron Microscope (ESEM) was used in this work. The EDX spectrometer is an EDAX PV7761/54 ME spectrometer with a Si(Li) detector of an active area of 30 mm and ATW2 window, which allows X-ray detection from elements higher than beryllium ($Z>4$). The system is equipped with "Genesis" hardware and software (EDAX, Inc) for computer-controlled SEM/EDX particle analysis. Using the CCSEM/EDX setup, a matrix of fields-of-view is set over the sample area, then the area is automatically inspected on a field-by-field basis. In each field-of-view particles are recognized by an increase of the detector signal above a pre-selected threshold level. After recognizing the particles in a field-of-view, the program acquires an X-ray spectrum from each detected particle. In this work, a magnification of 4000 × was used. Particles were imaged by acquiring the mixed signal of backscattered and transmitted electrons. Features with equivalent circle diameter larger than 0.2 μm were considered as particles by the software. The X-ray spectra were acquired for 5 s of clock time, at a beam current of 400–500 pA and an accelerating voltage of 20 kV. The relative dead times of the EDX spectrometer did not exceed 30%.

All samples were initially analyzed using SEM/EDX and CCSEM/EDX prior to exposure to nitric acid vapor. The samples were then transferred from the microscope to a flow reactor where they were exposed to nitric acid vapor. After the exposure, the samples were transferred back to the microscope where the same individual particles were analyzed again in order to detect consequential changes in their morphology and chemical composition.

Particles were exposed to nitric acid vapor in a flow reactor that has been described in detail elsewhere (Krueger et al., 2003b). The exposure conditions used in this work were $38 \pm 4\%$ RH, $p_{HNO_3} = 15 \pm 2\,\mu Torr$ (4.6×10^{11} molecules cm^{-3}), with dry nitrogen as a carrier gas. Total pressure in the reactor was set to 80 ± 2 Torr. Each type of the dust was exposed for 3 h. The partial pressure of nitric acid used in this study is equivalent to 20 ppb relative to atmospheric pressure which is adequate to level 10–20 ppb of nitric acid reported in polluted environments (Hering et al., 1988).

3. Results and discussion

3.1. Average elemental composition of different dust source regions determined from single particle analysis

Mineral dust samples from four different desert regions of the world were examined in this study. Fig. 1 displays the source regions of these samples along with digital images of the corresponding bulk samples. Even visual comparison of the dust color in the four images indicates a different mineralogy makeup for each of the samples. Since mineral dust entrained in the atmosphere is typically in the micron size range, the dust samples used in our study were purposely prepared to remove the larger particles, as described above. Thus, the mineral composition of these samples may not be identical to composition of the bulk dust from the specific region but may be representative of the mineral dust aerosol from these sources.

Computer-controlled analysis was used to determine the elemental composition of individual mineral dust particles. The average elemental composition of the dust samples determined from the analysis of thousands (1000–2000) of single particles is presented in Table 1. The compositions are represented as atomic percents of the following crustal elements Si, Al, Mg, Ca, Na and Fe. The data in Table 1 are listed as both average

Table 1
Average chemical composition of mineral dust particles from four source regions

Atomic percent	%Si	%Al	%Mg	%Ca	%Na	%Fe	%K
Mineral dust							
(a) Saharan	46	17	6	17	2	7	3
(b) Coastal Saudi	69	15	3	2	2	5	2
(c) Inland Saudi	53	22	7	3	2	9	3
(d) China Loess	31	7	13	39	4	3	1
Mineral dust							
Atomic fraction relative to Si	Si:Si	Al:Si	Mg:Si	Ca:Si	Na:Si	Fe:Si	K:Si
(a) Saharan	1	0.37	0.12	0.37	0.05	0.15	0.07
(b) Coastal Saudi	1	0.22	0.04	0.03	0.02	0.07	0.02
(c) Inland Saudi	1	0.41	0.14	0.06	0.03	0.17	0.05
(d) China Loess	1	0.23	0.42	1.25	0.14	0.10	0.04

composition in atomic percent and atomic fraction relative to Si. The crustal elements Si, Al, Mg, Ca, Na and Fe are all present in each sample, however, they are found in different proportions. Smaller amounts, $\leqslant 1\%$, of other elements such as V, K and Ti were also observed but are not listed in Table 1 and is the reason why the percentages do not total to 100 in Table 1.

As can be seen from the data in Table 1, the compositions of the mineral dusts from the four regions are distinctly different. For example, the data in Table 1 show that mineral dust from the Sahara desert contains the largest amount of Si and very little Ca. The China Loess sample contains less Si and greater amounts of Ca compared to the Sahara dust. Both of these dusts contain approximately similar amounts of Al. The Ca component of both dust sources is determined to be mostly from carbonate minerals including calcite and dolomite. The results reported here are in reasonable agreement with what has been reported in the literature for these various dust source regions (Aba-Husayn and Sayegh, 1977; Gallet et al., 1996; Nishikawa et al., 2000; Goudie and Middleton, 2001; Eltayeb et al., 2001; Falkovich et al., 2001; Caquineau et al., 2002; Formenti et al., 2003).

The inland dust from Saudi Arabia has the greatest Fe content which is the reason why the dust has a reddish hue in the digital image shown in Fig. 1. The coastal dust from Saudi Arabia has somewhat unique mineralogy in that it contains the largest components of Ca, Mg and Na relative to the other sources. This is in part due to the fact that there may be some sea salt mixed in with the dust due to its source location close to the Red Sea. As will be shown in the next section, the Ca component of the coastal dust from Saudi Arabia contains a large component of calcite due to natural sedimentation of carbonate concentrations in this region (El-Sayed et al., 2002) as well as gypsum, a sulfate mineral ($CaSO_4 \cdot 2H_2O$). These two calcium-containing minerals, calcite and gypsum, have very different reactivity toward nitric acid vapor.

3.2. Reactivity of individual mineral dust particles with nitric acid

Examples of the reactivity of individual dust particles from the China Loess sample are shown in Figs. 2 and 3. Each of these figures shows SEM images before and after reaction with nitric acid along with an EDX spectrum identifying the chemical nature of the labeled particles. The results show that carbonate-containing minerals, calcite in Fig. 2 (particle labeled b) and dolomite in Fig. 3 (particle labeled a), show unique morphology changes upon reaction with nitric acid. Although there are many fewer calcium-carbonate containing particles in the Sahara dust sample, the particles identified as calcite show identical morphology changes as that seen in the China Loess sample. These morphology changes have been observed previously for commercial calcite samples and are due to the formation of the calcium nitrate product, according to the bulk reaction, $CaCO_3+2HNO_3 \rightarrow Ca(NO_3)_2+CO_2+H_2O$. The nitrate product is very hygroscopic and undergoes deliquescence at low relative humidity ~10% RH 295 K (Tang and Fung, 1997; Al-Abadleh et al., 2003). Once calcium nitrate is deliquesced it retains its liquid, droplet-like shape even at the high vacuum of the SEM chamber and is the reason for the observed morphology changes. The resultant aqueous layer allows for continued reactivity of the carbonate particle without surface saturation and provides unrestricted transport of reactant (HNO_3) and product (CO_2) molecules in and out of this layer. Thus the bulk of the carbonate particle is available for reaction, making the reaction of nitric acid and calcium carbonate particle an important

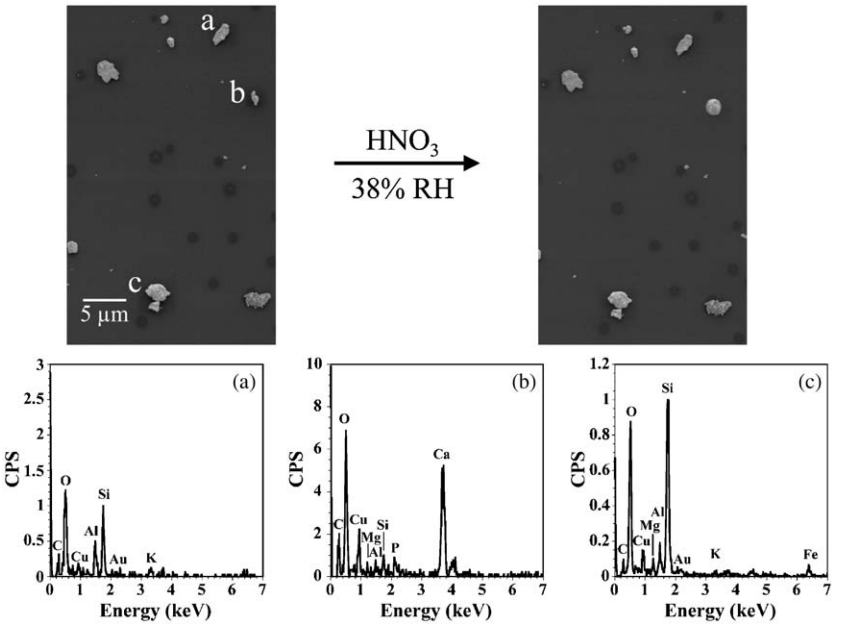

Fig. 2. SEM images of individual particles of China Loess are shown before and after exposure to nitric acid vapor at 38% RH. The EDX spectra for several individual particles (labeled a, b and c) prior to nitric acid exposure are also shown. Particles identified as an aluminum silicate clay (particle a) and quartz (particle c) show no change in morphology upon exposure to nitric acid. The particle labeled b with high levels of Ca is identified as $CaCO_3$. This particle shows unique morphological changes after reaction with nitric acid due to the formation of $Ca(NO_3)_2$, a hygroscopic salt. (*Note*: Trace amounts of Cu and Au in the EDX spectra are due to background signals from the sample holder and grid.)

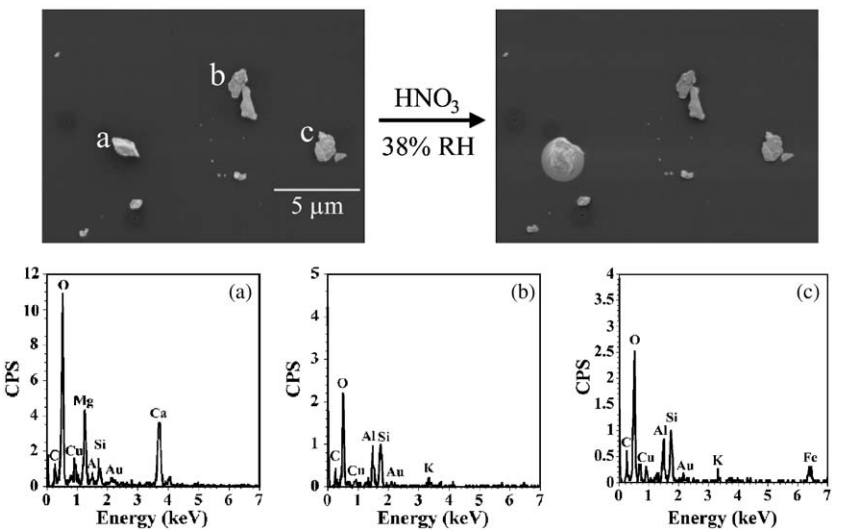

Fig. 3. (a–c) SEM images of individual particles of China Loess are shown before and after exposure to nitric acid vapor at 38% RH. The EDX spectra for several individual particles (labeled a, b and c) prior to nitric acid exposure are also shown. The particle labeled a with high levels of Ca and Mg is identified as dolomite, $CaMg(CO_3)_2$. This particle shows unique morphological changes after reaction with nitric acid consistent with the formation of a hygroscopic nitrate salt. The other particles identified as aluminum silicates (b and c) show no change in morphology upon exposure to nitric acid. (*Note*: Trace amounts of Cu and Au in the EDX spectra are due to background signals from the sample holder and grid.)

atmospheric chemical process (Tang et al., 2004; Song and Carmichael, 2001).

The other particles seen in Figs. 2 and 3 are mainly quartz and aluminum silicate clays. These particles do not show the same type of reactivity as is seen for carbonate particles. This suggests that either these particles are not reactive toward nitric acid or the reaction is surface limited and therefore not detected with the bulk-sensitive techniques used in this study.

The two different dust samples from Saudi Arabia show very different chemical composition and mineralogy with respect to the other dust samples and each other. As noted above, the inland Saudi Arabian dust shows three times the amount of Fe as the coastal dust whereas the coastal dust shows much larger amounts of Ca, Mg and Na. The coastal Saudi Arabian dust is extremely interesting from the perspective that there is a large component of the dust that contains calcium and thus many particles have the potential to be very reactive with respect to nitric acid. However, because of differences in the mineralogy, not all of the calcium-containing particles react similarly. The SEM/EDX data in Fig. 4 demonstrates this point. Fig. 4 shows an SEM image and five elemental maps (Ca, Mg, Si, N and S) of different particles from the coastal Saudi Arabian dust sample. Each of these particles contains high levels of calcium. Two of the particles also contain large amounts of sulfur. The particles that contain sulfur (particles labeled a and b) are associated with gypsum. The two other particles (particles labeled c and d) do not contain significant amounts of sulfur and therefore are carbonate particles. The elemental maps show some magnesium and silicon are observed in these particles as well. Nitrogen is not observed in any of the particles prior to exposure to nitric acid vapor.

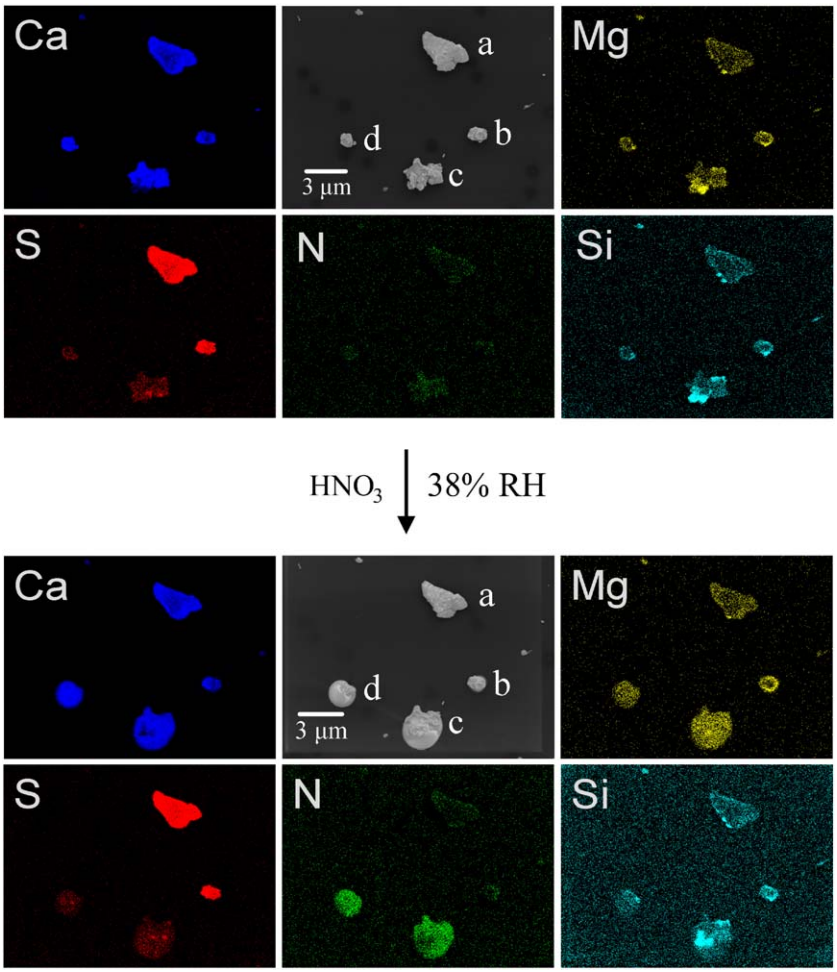

Fig. 4. SEM image and elemental mapping of individual calcium-containing particles (labeled a–d) of coastal Saudi Arabian dust prior to and after exposure to nitric acid at 38% RH. Five elemental maps are shown; these include Ca, Mg, S, N and Si. Particles labeled a and b are identified as calcium sulfate, gypsum. Particles labeled c and d are identified primarily as $CaCO_3$, calcite, although there is also some Si and Mg in the particle labeled c indicating this particle is a mineral aggregate.

The SEM/EDX data of these particles after reaction with nitric acid are also shown in Fig. 4. Several important conclusions can be drawn from the data shown in Fig. 4. It is evident from the SEM image that calcium particles that also contain sulfur do not change morphology upon reaction. The nitrogen content of the calcium sulfate particles also does not increase upon reaction indicating that these particles are not reactive towards nitric acid whereas the carbonate particles increase in nitrogen content. These results are consistent with the thermochemistry of these reactions. For the reaction, $CaCO_3(s) + 2HNO_3(g) \rightarrow Ca(NO_3)_2(s) + CO_2(g) + H_2O(l)$, ΔG is negative and equal to $-98.2\,kJ\,mol^{-1}$ whereas for the reaction, $CaSO_4(s) + 2HNO_3(g) \rightarrow Ca(NO_3)_2(s) + H_2SO_4(l)$, ΔG is positive and equal to $+36.2\,kJ\,mol^{-1}$. The $Ca(NO_3)_2$ solid then undergoes deliquescence at the relative humidities used in this study.

The elemental maps also show that some of these particles are mineral aggregates and contain other minerals as well. For example, one of the particles (the particle labeled c) contains a region with silicon but no calcium. After reaction with nitric acid, it can be seen that the reacted particle has little nitrogen content in the region that contains silicon whereas the rest of the particle does contain nitrogen. The data also show that the silicon portion of the particle becomes wetted and entrapped by the calcium nitrate solution. It is important to note that only techniques that incorporate imaging and chemical analysis such as the one used here can get at the detailed information on particle heterogeneity and reactivity demonstrated in this study.

Since these experiments were run with computer-controlled analysis, a statistical number of particles can be examined in ternary plots. The CCSEM/EDX results of particles containing >10% Ca before and after reaction are shown in ternary plots (a) Ca/S/O and (b) Ca/N/O in Fig. 5. In the ternary plots, the compositions are normalized such that the three elements specified total 100%. In Fig. 5a, the Ca/S/O plots show that particles containing <15% sulfur have a clear change in composition, with increasing oxygen content, compared to particles containing >15% sulfur. This is consistent with results reported above, i.e. calcium sulfate particles are not very reactive whereas calcium-containing carbonate particles are. As calcium carbonate particles react to form nitrate, the oxygen content doubles. This accounts for the shift in the ternary plots to higher concentrations of oxygen for particles with a sulfur content below 15%. The average oxygen content for particles with a sulfur content <15% increases by 10% for all the particles whereas the average oxygen content stays nearly constant for particles with a sulfur content >15%. In Fig. 5b, the C/N/O ternary plots show that there is little nitrogen content in the particles before reaction. The average nitrogen content increases by a factor of 3 after reaction with nitric acid. The oxygen content also increases.

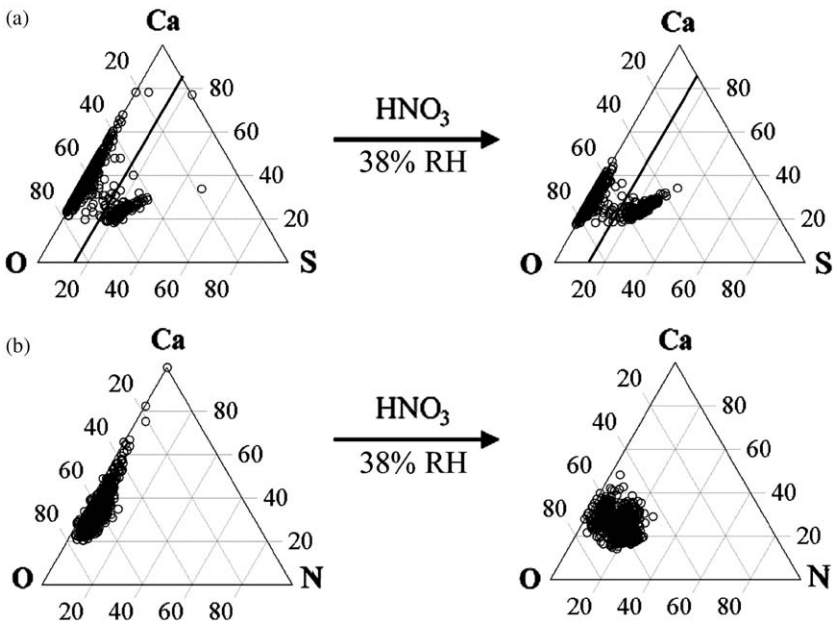

Fig. 5. Ternary plots of individual particles from coastal Saudi sand. Particles that contain >10% Ca are shown before and after exposure to nitric acid vapor at 38% RH: (a) Ca/S/O ternary plot and (b) Ca/N/O ternary plot. The line drawn through (a) is to guide the eye and represents particles that contain 15% sulfur, as there appears to be a clear change in composition, with respect to increasing oxygen content, for particles that contain <15% sulfur compared to particles containing more than 15% sulfur.

4. Conclusions and atmospheric implications

In this study, using individual particle analysis that allows for imaging and chemical analysis, we have shown that dust particle reactivity depends on the mineralogy of individual particles. The carbonate component of the dust is particularly reactive. In terms of the percentage of reactive particles, the two most reactive dust sources in this study are China Loess and coastal Saudi Arabia sand. This is because a large number of the calcium particles are associated with carbonate minerals. In the case of the coastal sand from Saudi Arabia, some of the calcium-containing particles are sulfate particles (e.g. gypsum). Gypsum is found to be unreactive towards nitric acid at 38% RH. From the elemental analysis, it is estimated that approximately 25% of the calcium-containing particles are gypsum. Based on the results reported in this study, it is clear that chemical composition and mineralogy should be included in atmospheric chemistry models that include heterogeneous chemistry because reaction on mineral dust aerosol would be poorly represented by a single kinetic parameter.

Although the need to have a detailed assessment of the mineral dust composition and its mineralogy in atmospheric models has been acknowledged (Sokolik et al., 2001) and discussed (Usher et al., 2003), this has been largely ignored in atmospheric chemistry models. As a first attempt at this, a percentage of particles with different reactivities may be considered. In particular, it is shown here that carbonate-containing minerals should be explicitly considered in the models because of their unique reactivity at least with respect to nitric acid in the atmosphere. These particles are an effective sink of nitric acid and their reactions with nitric acid are not surface limited and involve entire particle. The conversion of calcium carbonate to calcium nitrate may be a chemical marker for heterogeneous chemistry. Due to the formation of the deliquesced nitrate product in the aged particles, the uptake of nitric acid and other gas-phase pollutants (e.g. SO_2, NO_y HO_x, O_3, organics, etc) may perhaps be enhanced by orders of magnitude. In turn, aqueous chemistry in the deliquescent coating will take place, e.g. uptake of SO_2 into particle droplets followed by its oxidation to sulfate. In addition, optical properties and the ability to serve as an effective CCN will be also greatly enhanced in the aged carbonate particles.

Acknowledgements

The authors acknowledge support provided by the Biological and Environmental Research Program (BER), U.S. Department of Energy, Grant no. DE-FG01-98ER62580, and the National Science Foundation, through Grant no. CHE-9988434. This research was performed in the Environmental Molecular Sciences Laboratory, a national scientific user facility sponsored by the Department of Energy's Office of Biological and Environmental Research and located at Pacific Northwest National Laboratory. Pacific Northwest National Laboratory is operated by the U.S. Department of Energy by Batelle Memorial Institute under contract No. DE-AC06-76RL0 1830.

References

Aba-Husayn, M.M., Sayegh, A.H., 1977. Mineralogy of Al-Hasa desert soils (Saudi Arabia). Clay and Clay Minerals 25, 138–147.

Al-Abadleh, H.A., Krueger, B.J., Ross, J. L., Grassian, V.H., 2003. Phase transitions in calcium nitrate thin films. Chemical Communications 2796–2797.

Bauer, S.E., Balkanski, Y., Schulz, M., Hauglustaine, D.A., Dentener, F., 2004. Global modeling of heterogeneous chemistry on mineral aerosol surfaces: influence on tropospheric ozone chemistry and comparison to observations. Journal of Geophysical Research 109, D02304, doi:10.1029/2003JD003868.

Bian, H.S, Zender, C.S., 2003. Mineral dust and global tropospheric chemistry: relative roles of photolysis and heterogeneous uptake. Journal of Geophysical Research 108, 4672, doi:10.1029/2002JD003143.

Buseck, P.R., Pósfai, M., 1999. Airborne minerals and related aerosol particles: effects on climate and the environment. Proceedings of the National Academy of Science USA 96, 3372–3379.

Caquineau, S., Gaudichet, A., Gomes, L., Legrand, M., 2002. Mineralogy of Saharan dust transported over northwestern tropical Atlantic Ocean in relation to source regions. Journal of Geophysical Research 107, doi:10.1029/2000JD000247.

Claquin, T., Schulz, M., Balkanski, Y.M., 1999. Modeling the mineralogy of atmospheric dust sources. Journal of Geophysical Research 104, 22,243–22,256.

Dentener, F.J., Carmichael, G.R., Zhang, Y., Lelieveld, J., Crutzen, P.J., 1996. Role of mineral aerosol as a reactive surface in the global troposphere. Journal of Geophysical Research 101, 22,869–22,890.

Dickerson, R.R., Kondragunta, S., Stenchikov, G., Civerolo, K.L., Doddridge, B.G., Holben, B.N., 1997. The impact of aerosols on solar ultraviolet radiation and photochemical smog. Science 278, 827–830.

El Sayed, M.A., Basaham, A.S., Gheith, A.M., 2002. International Journal of Environmental Studies 59, 1–31.

Eltayeb, M.A.H., Injuk, J., Maenhaut, W., Van Grieken, R.E., 2001. Elemental composition of mineral aerosol generated from Sudan Sahara sand. Journal of Atmospheric Chemistry 40, 247–273.

Falkovich, A.H., Ganor, E., Levin, Z., Formenti, P., Rudich, Y., 2001. Chemical and mineralogical analysis of individual mineral dust particles. Journal of Geophysical Research 106, 18,029–18,036.

Formenti, P., Elbert, W., Maenhaut, W., Haywood, J., Andreae, M.O., 2003. Inorganic and carbonaceous aerosols

during the Southern African Regional Science Initiative (SAFARI 2000) experiment: chemical characteristics, physical properties, and emission data for smoke from African biomass burning. Journal of Geophysical Research 108, 8576.

Gallet, S., Jahn, B.-M., Torii, M., 1996. Geochemical characterization of the Luochuan loess-paleosol sequence, China, and paleoclimatic implications. Chemical Geology 133, 67–88.

Garçon, G., Shirali, P., Sébastien, G., Fontaine, M., Zerimech, F., Martin, A., Hannothiaux, M.-H., 2000. Polycyclic aromatic hydrocarbon coated onto Fe_2O_3 particles: assessment of cellular membrane damage and antioxidant system disruption in human epithelial lung cells (L132) in culture. Toxicology Letters 117, 25–35.

Goudie, A.S., Middleton, N.J., 2001. Saharan dust storms: nature and consequences. Earth-Science Reviews 56, 179–204.

Guthrie Jr., G.D., Mossman, B.T., 1993. Merging the geological and biological sciences; an integrated approach to the study of mineral-induced pulmonary diseases. In: Guthrie Jr., G.D., Mossman, B.T. (Eds.), Health Effects of Mineral Dust, vol. 28. Reviews in Mineralogy, Mineralogical Society of America. Washington, DC, pp. 1–5.

Hering, S.V., Lawson, D.R., Allegrini, I., Febo, A., Perrino, C., Possanzini, M., J.E. Sickles, I., Anlauf, K.G., Wiebe, A., Appel, B.R., John, W., Ondo, J., Wall, S., Braman, R.S., Sutton, R., Cass, G.R., Solomon, P.A., Eatough, D.J., Eatough, N.L., Ellis, E.C., Grosjean, D., Hicks, B.B., Womack, J.D., Horrocks, J., Knapp, K.T., Ellestad, T.G., Paur, R.J., Mitchell, W.J., Pleasant, M., Peake, E., MacLean, A., Pierson, W.R., Brachaczek, W., Schiff, H.I., Mackay, G.I., Spicer, C.W., Stedman, D.H., Winer, A.M., Biermann, H.W., Tuazon, E.C., 1988. The nitric acid shootout—field comparison of measurement methods. Atmospheric Environment 22, 1519–1539.

Krueger, B.J., Grassian, V.H., Laskin, A., Cowin, J.P., 2003a. The transformation of solid atmospheric particles into liquid droplets through heterogeneous chemistry: laboratory insights into the processing of calcium containing mineral dust aerosol in the troposphere. Geophysical Research Letters 30, doi:10.1029/2002GL016563.

Krueger, B.J., Grassian, V.H., Iedema, M.J., Cowin, J.P., Laskin, A., 2003b. Probing heterogeneous chemistry of individual atmospheric particles using scanning electron microscopy. Analytical Chemistry 75, 5170–5179.

Levin, Z., Ganor, E., Gladstein, V., 1996. The effects of desert particles coated with sulfate on rain formation in the eastern Mediterranean. Journal of Applied Meteorology 35, 1511–1523.

Liao, H., Adams, P.J., Chung, S.H., Seinfeld, J.H., Mickley, L.J., Jacob, D.J., 2003. Interactions between tropospheric chemistry and aerosols in a unified general circulation model. Journal of Geophysical Research 108, doi:10.1029/2001JD001260.

Mahowald, N.M., Kiehl, L.M., 2003. Mineral aerosol and cloud interactions. Geophysical Research Letters 30 (9), 1475.

Martin, S.T., 2000. Phase transitions of aqueous atmospheric particles. Chemical Reviews 100, 3403–3453.

Martin, R.V., Jacob, D.J., Yantosca, R.M., Chin, M., Ginoux, P., 2003. Global and regional decreases in tropospheric oxidants from photochemical effects of aerosols. Journal of Geophysical Research 108 (D3), 4097.

Meskhidze, N., Chameides, W.L., Nenes, A., Chen, G., 2003. Iron mobilization in mineral dust: can anthropogenic SO_2 emissions affect ocean productivity? Geophysical Research Letters 2058, doi: 10.1029/2003GL018035.

Nishikawa, M., Hao, Q., Morita, M., 2000. Global Environmental Research 4, 103–113.

Prospero, J.M., Ginoux, P., Torres, O., Nicholson, S.E., Gill, T.E., 2002. Environmental characterization of global sources of atmospheric soil dust identified with the Nimbus 7 Total Ozone Mapping Spectromete (TOMS) absorbing aerosol production. Reviews of Geophysics 40 (1), 1002.

Rosenfield, D., Rudich, Y., Lahav, R., 2001. Desert dust suppressing precipitation: a possible desertification feedback loop. Proceedings of the National Academy of Sciences-USA 1998, 5975–5980.

Rudich, Y., Khersonsky, O., Rosenfeld, D., 2002. Treating clouds with a grain of salt. Geophysical Research Letters 29 (22), 2060.

Rudich, Y., Sagi, A., Rosenfeld, D., 2003. Influence of the Kuwait oil fires plume (1991) on the microphysical development of clouds. Journal Geophysical Research 108 (D15), 4478.

Sassen, K., DeMott, P.J., Prospero, J.M., Poellot, M.R., 2003. Saharan dust storm and indirect aerosol effects on clouds: CRYSTAL-FACE results. Geophysical Research Letters 30 (12), 1633.

Sokolik, I.N., Winker, D.M., Bergametti, G., Gillette, D.A., Carmichael, G., Kaufman, Y.J., Gomes, L., Schuetz, L., Penner, J.E., 2001. Introduction to special section: outstanding problems in quantifying the radiative impacts of mineral dust. Journal of Geophysical Research 106, 18,015–18,027.

Song, C.H., Carmichael, G.R., 2001. Gas-particle partitioning of nitric acid modulated by alkaline aerosol. Journal of Atmospheric Chemistry 40, 1–22.

Tang, I.N., Fung, K.H., 1997. Hydration and Raman scattering studies of levitated microparticles: $Ba(NO_3)_2$, $Sr(NO_3)_2$, and $Ca(NO_3)_2$. Journal of Chemical Physics 106, 1653–1660.

Tang, Y., Carmichael G.R., Kurata, G., Uno, I., Weber, R.J., Song, C.-H., Guttikunda, S.K., Woo, J.-H., Streets, D.G., Wei, C., Clarke, A.D., Huebert, B., Anderson, T.L., 2004. The impacts of dust on regional tropospheric chemistry during the ACE-Asia experiment: a model study. Journal of Geophysical Research, in press.

Tegen, I., 2003. Modeling the mineral dust aerosol cycle in the climate system. Quaternary Science Reviews 22, 1821–1834.

Toon, O.B., 2003. Atmospheric science—African dust in Florida clouds. Nature 424, 623–624.

Usher, C.R., Michel, A.E., Grassian, V.H., 2003. Reactions on mineral dust. Chemical Reviews 103, 4883–4940.

Yin, Y., Wurzler, S., Levin, Z., Reisin, T.G., 2002. Interactions of mineral dust particles and clouds: effects on precipitation and cloud optical properties. Journal of Geophysical Research 107 (D23), 4724.

Zhu, X., Prospero, J.M., Savoie, D.L., Millero, F.J., Zika, R.G., Saltzman, E.S., 1993. Photoreduction of iron (III) in marine mineral aerosol solutions. Journal of Geophysical Research 98, 9039–9046.